CHEMISTRY
A EUROPEAN JOURNAL

DOI: 10.1002/chem.200801889

Stereoselective Allylation of Ketones: Explanation for the Unusual Inversion of the Induced Stereochemistry in the Auxiliary-Mediated Crotylation and Pentenylation of Butanone by DFT Calculations

Lutz F. Tietze,*[a] Tom Kinzel,[a] and Stefan Schmatz[b]

Dedicated to Professor Armin de Meijere on the occasion of his 70th birthday

Abstract: Auxiliary-mediated domino crotylations and pentenylations of butanone yield homoallylic ethers with two newly formed stereogenic centers. With our norpseudoephedrine-derived auxiliary, we observed the formation of *anti* isomers exclusively, and the nature of the major isomer was independent of the substrate double bond geometry. Interestingly, there is a switch in induced selectivity when going from crotylation to pentenylation. Here, we present the computational rationalization for this behavior by identification of the relevant transition states (TSs), the energies of which were determined by using the B3LYP/6-31+G(d) level of theory in combination with the PCM/UAKS method to include the effects exerted by the solvent dichloromethane. To quickly narrow down the number of potentially relevant TSs from the whole set of 288 and 864 TSs for the crotylation and pentenylation, respectively, we employed a screening process based on B3LYP//AM1 energies. The predicted selectivities are in good agreement with experimentally determined ones. Furthermore, the obtained results also facilitate an explanation of the selectivities obtained in hexenylations and heptenylations. Finally, activation energies were determined that account for the significantly longer reaction times than those for the domino allylation with unsubstituted trimethylallylsilane.

Keywords: allylation · chiral auxiliaries · density functional calculations · diastereoselectivity · norpseudoephedrine

Introduction

Homoallylic alcohols and ethers are versatile building blocks in organic synthesis. While many catalytic methods exist for the asymmetric allylation of aldehydes,[1] the stereoselective allylation of ketones is still a very challenging task.[2] We have developed an auxiliary-based domino[3] method in which a methyl ketone such as butanone (**1**) reacts together with allyltrimethylsilane (**2a**) and the norpseudoephedrine-derived silyl ether (*S*,*S*)-**3** in the presence of catalytic amounts of trifluoromethanesulfonic acid (TfOH) to give homoallylic ethers such as **4a** (Scheme 1).[4] The transferred auxiliary moiety can be cleaved by using, for example, Birch conditions[5] to afford the desired homoallylic alcohol in high optical purity. With this method, even the differentiation between a methyl and an ethyl group in **1** is possible with a diastereomeric ratio of 90:10 at −78 °C (Table 1, entry 1).

We have expanded the scope of the reaction by employing both *E*- and *Z*-configured γ-substituted allyl silanes (**2b–e**) (Table 1, entries 2–9).[6] In each case, only two out of the four possible isomers of **4b–e** are formed (in the following, termed major and minor isomer). Regardless of the double bond geometry of the silane, the main and minor isomers of **4b–e** are always 3,4-*anti*-configured. This is in line with our study on the crotylation of aldehydes and ketones with *E*- and *Z*-configured crotyl silanes in the presence of TMSOMe.[7] Moreover, the absolute stereochemistry of the formed isomers is independent of the silane double bond geometry as well. Interestingly, there is an unexpected switch

[a] Prof. Dr. Dr. h. c L. F. Tietze, Dr. T. Kinzel
Institut für Organische und Biomolekulare Chemie
Georg-August-Universität Göttingen
Tammannstrasse 2, 37077 Göttingen (Germany)
Fax: (+49) 551-399476
E-mail: ltietze@gwdg.de

[b] Prof. Dr. S. Schmatz
Institut für Physikalische Chemie
Georg-August-Universität Göttingen
Tammannstrasse 6, 37077 Göttingen (Germany)

Supporting information for this article is available on the WWW under http://dx.doi.org/10.1002/chem.200801889.

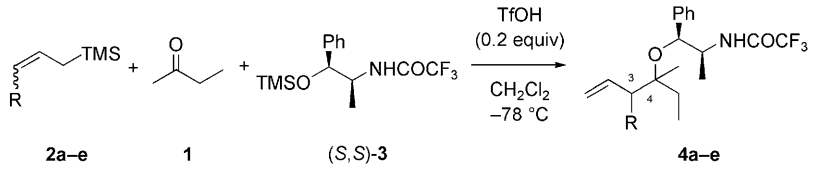

2a–e 1 (*S*,*S*)-**3** **4a–e**

Scheme 1. Allylation of butanone for the stereoselective formation of homoallylic ethers.

Table 1. Selectivities and configuration of the main isomer for the allylation of butanone with unsubstituted and γ-substituted allyl silanes.

Entry	Allyl silane	R	*E*/*Z*	Product	Selectivity (^{13}C NMR)	Main isomer of **4** (X-ray)
1	**2a**	H	–	**4a**	90:10	4*R*
2	(*E*)-**2b**	Me	*E*	**4b**	90:10	3*S*,4*R*
3	(*Z*)-**2b**	Me	*Z*	**4b**	75:25	3*S*,4*R*
4	(*E*)-**2c**	Et	*E*	**4c**	70:30	3*R*,4*S*
5	(*Z*)-**2c**	Et	*Z*	**4c**	86:14	3*R*,4*S*
6	(*E*)-**2d**	*n*Pr	*E*	**4d**	82:18	3*R*,4*S*
7	(*Z*)-**2d**	*n*Pr	*Z*	**4d**	93:7	3*R*,4*S*
8	(*E*)-**2e**	*n*Bu	*E*	**4e**	85:15	3*R*,4*S*
9	(*Z*)-**2e**	*n*Bu	*Z*	**4e**	95:5	3*R*,4*S*

in the induced selectivity when going from crotyl silanes (**2b**) to longer chained silanes (**2c**–**e**).

Recently, we were able to elucidate the origin of the high stereoselectivity of the allylation with **2a** by a systematic computational study of all possible transition state (TS) geometries.[8] We assumed the stereogenic step to be the nucleophilic attack of allyl silane on an intermediate oxocarbenium ion **5** (Scheme 2). This mechanism is substantiated by the results of a number of experimental and computational studies.[9]

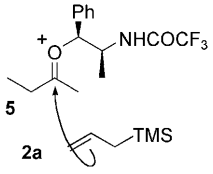

Scheme 2. Proposed stereogenic step for the auxiliary-mediated allylation of butanone.

The systematic consideration of the conformational degrees of freedom for the system **2a**+**5** leads to 288 possible TS conformations. To deal with this large number, we have developed a procedure based on B3LYP//AM1 energies to quickly select potentially relevant TSs before performing time-consuming calculations at the final DFT level. Thus, we were able to narrow down the size of the final set of TSs to 61, from which 14 relevant TSs were identified. These TSs can be grouped by *Re*- or *Si*-face attack to the oxocarbenium ion **5** in conformations $\mathbf{5_1}$, $\mathbf{5_2}$, or $\mathbf{5_3}$ (Scheme 3). The predicted selectivity of 85:15 is in excellent agreement with the experimental value of 90:10.

The order of the TS energies is a result of two competing effects: Intra-TS steric interactions are minimized with conformation $\mathbf{5_3}$ (in all relevant TSs in the gas phase, **5** exclusively adopts this conformation), whereas the more compact TSs with conformations $\mathbf{5_1}$ and $\mathbf{5_2}$ become relevant in solution, because the surface accessible for the solvent molecules is only small. A simple 2-TS model cannot sufficiently explain the stereoinduction for this process.

In the present work, we adapted the computational approach to identify the relevant TSs for the allylation of butanone with γ-substituted allyl silanes to explain a) why the same isomer is formed when either *E*- or *Z*-configured silanes are employed, and b) why there is an inversion in stereoselectivity when going from crotylation to pentenylation. We selected three systems for a detailed study: The attack of the butanone-derived oxocarbenium ion **5** with *E*- and *Z*-configured crotyl silane ((*E*)-**2b** and (*Z*)-**2b**) (Table 1, entries 2 and 3), and the pentenylation of **5** with (*Z*)-pentenyl silane ((*Z*)-**2c**) (Table 1, entry 5). The agreement of the computationally predicted with the experimentally observed selectivites represents a strong validation of the assumed mechanism and the relevance of the calculated TS structures.

For simplification, only the descriptors of the stereogenic centers at C-3 and C-4 of **4b** and **4c** are given in the following; for example, (*RS*)-**4b** corresponds to (3*R*,4*S*,1′*S*,2′*S*)-**4b**.

Results and Discussion

Identification of relevant TSs: As in the allylation reaction with **2a**, there are 288 possible TS conformations for the crotylations with (*E*)-**2b** or (*Z*)-**2b**. This number is a result from attack of the *Re*- or *Si*-face of **2b** at the *Re*- or *Si*-face of the *E*- or *Z*-configured oxocarbenium ion **5** in one of three relative orientations of the double bonds in **2b** and **5** (antiperiplanar or one of two synclinal possibilities), in combination with several conformational degrees of freedom within **5**. This number increases by a factor of 3 to a total of 864 structures for the pentenylation with **2c**, since the ethyl group in the γ-position of the allyl silane may adopt one of

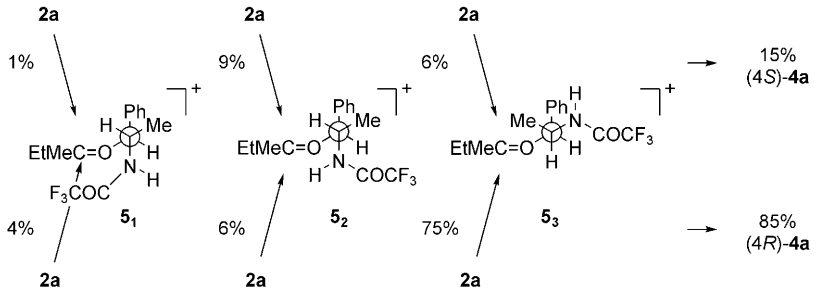

Scheme 3. Contribution of relevant TSs to the product formation of **4a** grouped by conformations $\mathbf{5_1}$, $\mathbf{5_2}$, and $\mathbf{5_3}$. In all relevant TSs, **5** has *E*-configuration.

three conformations relative to the position of the silyl group.

The aforementioned screening method allowed us to select 22, 24, and 33 potentially relevant TSs for the attack of (*E*)-**2b**, (*Z*)-**2b**, and (*Z*)-**2c**, respectively, by selecting all TSs with relative energies of less than 15 kJ mol^{-1} as determined by B3LYP/6-31+G(d)/PCM/UAKS single-point calculations on AM1-optimized geometries (see Computational Details). Relevant TSs are defined as having a relative free energy of less than 6 kJ mol^{-1} in relation to the lowest-energy TS; only relevant TSs may contribute significantly to product formation.

The sets of TSs were subjected to geometry optimization and frequency calculation at the B3LYP/6-31+G(d)/PCM/UAKS level of theory. In our previous studies on related systems, we found the inclusion of solvent effects in the optimization step to be essential.

Crotylation with (*E*)-2b: For the crotylation with (*E*)-**2b**, the six TSs displayed in Table 2 were found to be relevant. From their energies, an isomer ratio of *anti*-**4b**:*syn*-**4b** of

Table 2. Relevant TSs for the crotylation of butanone with (*E*)-crotylsilane (EC, (*E*)-**2b**). R = (*S*,*S*)-CH(CH$_3$)-NHCOCF$_3$.

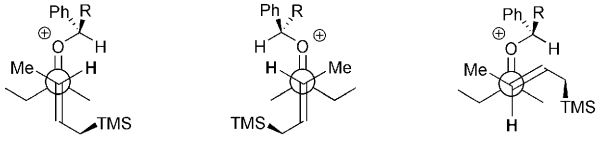

A → (*SR*)-**4b** B → (*RS*)-**4b** C → (*RR*)-**4b**

Stereoisomer	Trajectory	TS[a]	G_{rel} [kJ mol^{-1}]	c_{TS}[b] [%]	Isomer ratio [%] calcd[c]	exptl
(*SR*)-**4b**	A	**EC-A$_3$**	0.0	50.0	53 (78)	90
		EC-A$_2$	4.6	2.9		
(*RS*)-**4b**	B	**EC-B$_2$**	3.2	6.9	15 (22)	10
		EC-B$_1$	3.4	6.1		
		EC-B$_3$	5.7	1.5		
(*RR*)-**4b**	C	**EC-C$_3$**	0.7	32.4	32	-

[a] Subscripts 1, 2, and 3 denote the oxocarbenium ion geometry according to Scheme 3. [b] c_{TS} = TS contribution to product formation. [c] Values in parentheses correspond to the ratio of the *anti* isomers.

68:32 is calculated. While the amount of the *syn* isomer is overestimated, the calculation correctly predicts the *anti* isomer to be the main product. The ratio of the *anti* isomers (*SR*)-**4b**:(*RS*)-**4b** is predicted to be 78:22, which is very close to the experimental value of 90:10.

As in the allylation reaction with **2a**, in relevant TSs **5** is always *E*-configured and the side chain adopts one of the conformations **5$_{1-3}$** that are shown in Scheme 3. Concerning the relative orientation of (*E*)-**2b** and **5**, there are three attack trajectories A, B, and C shown in Table 2. In trajectories A and B, the double bonds adopt an antiperiplanar orientation with the methyl group in the γ-position pointing away from the auxiliary side chain. Apart from the chiral residue, A and B represent mirror images and lead to the *anti* isomers (*SR*)-**4b** and (*RS*)-**4b**, respectively. TSs **EC-A$_3$** and **EC-B$_2$** are shown in Figure 1. On the other hand, the TS **EC-C$_3$** with synclinal orientation of the double bonds is calculated to be energetically accessible although its product (*RR*)-**4b** is not observed in experiments.

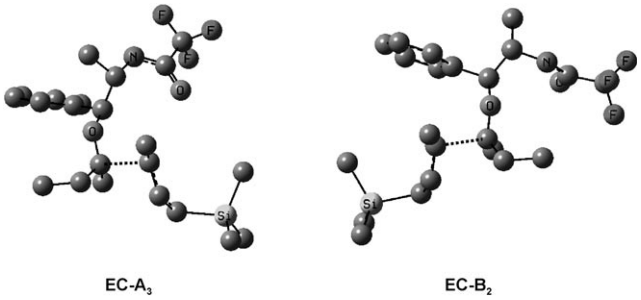

Figure 1. TSs **EC-A$_3$** and **EC-B$_2$** for the crotylation of butanone with (*E*)-**2b**. Hydrogen atoms are omitted for clarity.

Crotylation with (*Z*)-2b: Five TSs were found to be relevant for the crotylation with (*Z*)-**2b**, the energies of which translate to a predicted ratio of *anti*-**4b**:*syn*-**4b** of 98:2. The *anti* isomers (*SR*)-**4b**:(*RS*)-**4b** are predicted to be formed in a 59:41 ratio, which reproduces the experimental value of 75:25 well. Moreover, the trend of the crotylation with (*Z*)-**2b** being less selective than with (*E*)-**2b** is correctly reproduced.

Table 3 displays the TSs and their energies. As in the crotylation with (*E*)-**2b**, the formation of the *anti* isomers is predicted to proceed via TSs in which **5** adopts conformations **5$_1$**, **5$_2$**, or **5$_3$**, and where the double bonds of **5** and (*Z*)-**2b** adopt an antiperiplanar orientation. The most relevant TSs **ZC-A$_3$** and **ZC-B$_3$** are displayed in Figure 2.

Table 3. Relevant TSs for the crotylation of butanone with *Z*-crotylsilane (ZC, (*Z*)-**2b**). R = (*S*,*S*)-CH(CH$_3$)-NHCOCF$_3$.

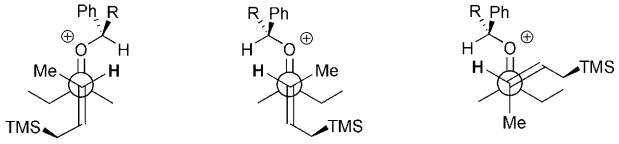

A → (*SR*)-**4b** B → (*RS*)-**4b** D → (*SS*)-**4b**

Stereoisomer	Trajectory	TS[a]	G_{rel} [kJ mol^{-1}]	c_{TS}[b] [%]	Isomer ratio [%] calcd	exptl
(*SR*)-**4b**	A	**ZC-A$_3$**	0.0	58.3	58	75
(*RS*)-**4b**	B	**ZC-B$_3$**	0.8	35.6	40	25
		ZC-B$_2$	5.0	2.7		
		ZC-B$_1$	5.9	1.5		
(*SS*)-**4b**	D	**ZC-D$_2$**	5.6	1.8	2	–

[a] Subscripts 1, 2, and 3 denote the oxocarbenium ion geometry according to Scheme 3. [b] c_{TS} = TS contribution to product formation.

Trajectories A and B for the crotylation with (*E*)-**2b** and (*Z*)-**2b** differ only in the position of the CH$_2$TMS group. In comparison to the TSs with (*E*)-**2b**, this introduces a subtle additional steric interaction with the ethyl group in **5** that

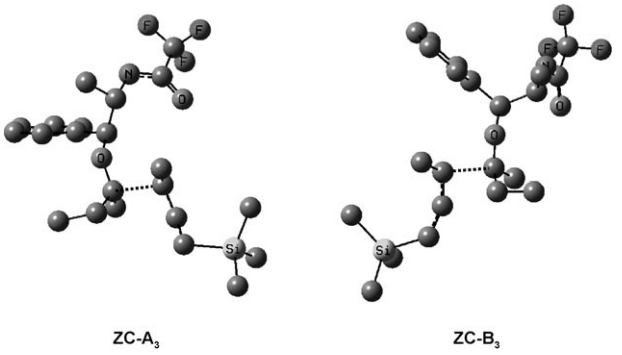

Figure 2. TSs **ZC-A$_3$** and **ZC-B$_3$** for the crotylation of butanone with (*Z*)-**2b**. Hydrogen atoms are omitted for clarity.

however applies uniformly to all relevant TSs, thus not changing the order of the TS energies. Consequently, the same main isomer is formed independent of the double bond geometry of **2b**.

Pentenylation with (*Z*)-2c: Of the 864 possible TSs for the pentenylation with (*Z*)-**2c**, only two were found to be of relevance, each leading to one of the experimentally observed *anti* isomers of **4c** (Table 4, Figure 3). In contrast to the crotylations, the attack at the *Re*-face of **5** via TS **ZP-B$_3$** is now favored, leading to a ratio of 29:71 which correctly reproduces the inversion of selectivity.

Table 4. Relevant TSs for the pentenylation of butanone with *Z*-pentenylsilane (ZP, (*Z*)-**2c**). R = (*S*,*S*)-CH(CH$_3$)-NHCOCF$_3$.

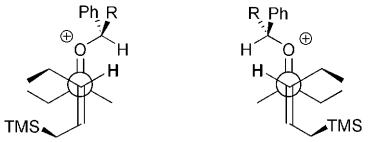

A → (*SR*)-**4c** B → (*RS*)-**4c**

Stereoisomer	Trajectory	TS[a]	G_{rel} [kJ mol^{-1}]	c_{TS}[b] [%]	Isomer ratio [%] calcd	exptl
(*SR*)-**4c**	A	**ZP-A$_3$**	1.4	29.2	29	14
(*RS*)-**4c**	B	**ZP-B$_3$**	0.0	70.8	71	86

[a] Subscript 3 denotes the oxocarbenium ion geometry according to Scheme 3. [b] c_{TS} = TS contribution to product formation.

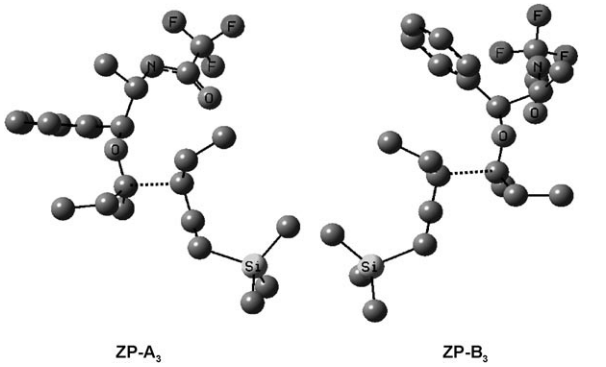

Figure 3. TSs **ZP-A$_3$** and **ZP-B$_3$** for the pentenylation of butanone with (*Z*)-**2c**. Hydrogen atoms are omitted for clarity.

Rationalization of TS energies: For a rationalization of the calculated relative free energies in solution, G_{rel}, steric and electronic effects within the TS must be separated from the free energy of solvation ΔG_{solv}. Our previous study has shown that differences in ΔG_{solv} have a pronounced impact on the energetic accessibility of certain groups of TSs.[8] Thus, we performed single-point calculations without the inclusion of solvent (gas phase) on the structures that were optimized in solution. Table 5 displays the resulting relative energy differences, G_{rel}^{GP}, and the relative energies of solvation, $\Delta G_{solv,rel}$, for all TSs with attack trajectories A and B. Additionally, the geometric parameters *d* (distance between the bond-forming carbons), α (Bürgi–Dunitz angle), γ (relative orientation of the double bonds in **5** and **2**), and δ (tilting of the auxiliary phenyl group in relation to the double bond in **5**), as defined in Figure 4, were measured for these TSs.

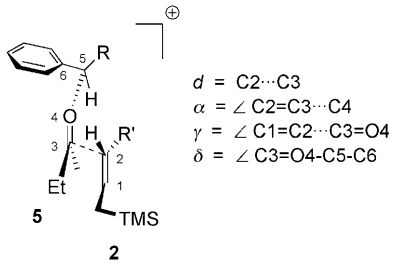

Figure 4. Selected geometric parameters for the description of TS conformations. R = (*S*,*S*)-CH(CH$_3$)-NHCOCF$_3$; R′ = Me, Et.

Inspection of Table 5 reveals that in the gas phase, only TSs in which **5** adopts conformation **5$_3$** are energetically accessible. This is simply explained by **5$_3$** being the conformation in which the distance between the auxiliary side chain and the approaching silane is maximized, thus leading to minimum steric interaction. Furthermore, *Si*-face attack of **5** via TSs **A$_3$** is favored over *Re*-face attack via TSs **B$_3$** which can be traced back to the loss of stereoelectronic stabilization of **5** by the phenyl group which needs to tilt away from about 94° in TSs **A$_3$** to about 125° in TSs **B$_3$**. The energy difference becomes less pronounced when going from (*E*)-**2b** to (*Z*)-**2b** or (*Z*)-**2c**, which might be due to the fact that the CH$_2$TMS group is further away from the auxiliary side chain in TSs with *Z*-configured silanes.

Upon solvation, all shown TSs gain relevance with respect to TSs **A$_3$**. On the one hand, TSs with conformations **5$_1$** and **5$_2$** become accessible for the crotylation systems; however, this stabilization is not sufficient to replace TSs with **5$_3$** as the most relevant TSs, therefore leading to an increased number of relevant TSs. This can be traced back to the compact nature of these TSs, resulting in a smaller solvent accessible surface and thus (relative) stabilization in the non-coordinating solvent dichloromethane. Furthermore, the TSs

Table 5. Energies and selected geometric parameters for TSs with attack trajectories A and B.

System	TS	G_{rel} [kJ mol^{-1}]	G_{rel}^{GP} [kJ mol^{-1}]	$\Delta G_{Solv,rel}$[a] [kJ mol^{-1}]	d [Å]	α [°]	γ [°]	δ [°]
5 + (*E*)-**2b**	**EC-A$_3$**	0.0	0.0	0.0	2.088	99.1	−174.4	95.3
	EC-A$_2$	4.6	12.3	−7.7	2.053	100.1	−173.3	82.3
	EC-B$_2$	3.2	14.9	−11.7	2.063	100.9	178.2	87.5
	EC-B$_1$	3.4	18.0	−14.6	2.085	100.3	177.2	78.4
	EC-B$_3$	5.7	9.4	−3.7	2.090	99.5	177.0	128.4
5 + (*Z*)-**2b**	**ZC-A$_3$**	0.0	0.0	0.0	2.047	100.3	−173.5	93.8
	ZC-B$_3$	0.8	4.1	−3.3	2.071	100.3	174.0	123.7
	ZC-B$_2$	5.0	12.6	−7.6	2.039	101.8	172.7	88.9
	ZC-B$_1$	5.9	16.6	−10.7	2.056	101.6	173.0	81.5
5 + (*Z*)-**2c**	**ZP-A$_3$**	0.0	0.0	0.0	1.989	101.2	−173.9	93.4
	ZP-B$_3$	−1.4	3.5	−4.9	1.998	101.3	173.4	121.1

[a] Relative free energy of solvation with ΔG_{Solv} for **A$_3$**-TSs arbitrarily set to 0 kJ mol^{-1} ($G_{rel} = G_{rel}^{GP} + \Delta G_{Solv,rel}$).

B$_1$ are additionally stabilized in solution because of their large dipole moment (≈15 D) in comparison to TSs with **5$_2$** or **5$_3$** (≈9 to 10 D).

On the other hand, TSs **B$_3$** are better stabilized than TSs **A$_3$** by 3.3–4.9 kJ mol^{-1}, which in the case of (*Z*)-**2c** is sufficient to replace **ZP-A$_3$** as the lowest-energy TS. Consequently, (*RS*)-**4c** is formed as main product, whereas in the case of crotylation, (*SR*)-**4b** is mainly formed. The change in relative energy is illustrated in Figure 5: A trend can be seen that helps to understand the selectivities with γ-substituted silanes: With some confidence, we may assume that

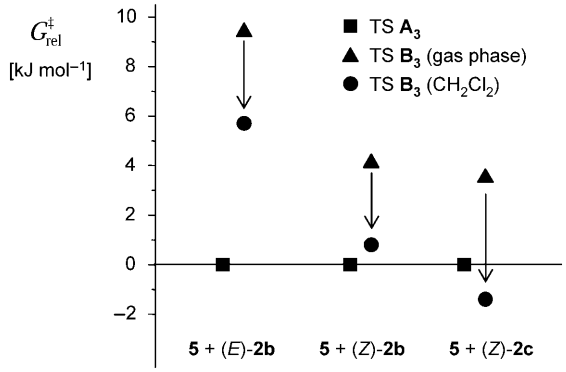

Figure 5. Relative energy change between TSs **A$_3$** and **B$_3$** when going from gas phase to solution.

the relevant TSs in allylations with **2d** and **2e** are also TSs **A$_3$** and **B$_3$**. The energy difference between TSs **A$_3$** and **B$_3$** increases further as the size of the substituent in the γ-position of **2** increases, leading to an even increased selectivity. The energy of TSs **B$_3$** remain larger in the case of *E*-configured silanes in relation to the corresponding TSs **A$_3$** (in absolute terms), leading to higher selectivity for the crotylation and lower selectivities in pentenylations, hexenylations, and heptenylations.

Activation energies: Activation energies were determined as the free energy difference between the sum of the ground states of **5** and **2**, and the lowest-energy TS. The thermodynamic correction term from the B3LYP/6-31+G(d)/PCM/UAKS calculation was added to the B3LYP/6–311++G(2d,p)/PCM/UAKS single-point energy on the geometries obtained with the smaller basis set. We found activation energies of 159.9, 156.2, and 165.8 kJ mol^{-1} for the reaction with (*E*)-**2b**, (*Z*)-**2b**, and (*Z*)-**2c**, respectively. These values are significantly higher than those for the allylation with **2a** (139.1 kJ mol^{-1})[8] and might explain why the reaction times need to be increased from 2 h with **2a** to several days with γ-substituted allyl silanes. On the other hand, the stereoselective step is not neccessarily also the rate-determining step of the homoallylic ether formation.

Experimental elucidation of the minor isomer stereochemistry: To assess the validity of the computational results, the predicted and observed ratios of both the main and minor isomer must be compared. In the original publication, only the major isomer stereochemistry was determined by X-ray crystallography, while the minor isomer was argued to be the second *anti* isomer by analogy reasoning.[6] Computational results for the crotylation with (*E*)-**2b** however predict the minor isomer to be (*RR*)-**4b** and not the originally published (*RS*)-**4b**, while the main isomer is correctly predicted to have (*SR*)-configuration.

To resolve the uncertainty concerning the minor isomer, we unambigously determined its absolute configuration: Under the assumption that the minor isomer is the predicted (*RR*)-isomer, we transformed the homoallylic ether mixture **4b** into allyl ethers **6** with one stereogenic center less (Scheme 4, a).[10] Allyl ether **6** proved to be a mixture of dia-

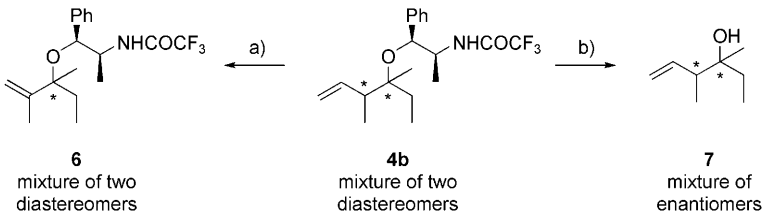

Scheme 4. Transformations of the homoallylic ether mixture for the determination of the minor isomer stereochemistry: a) 1. O_3, PPh_3, 96%; 2. $NaBH_4$, MeOH; 3. *o*-NO_2-C_4H_6-SeCN, then H_2O_2, 76% (2 steps). b) Na, NH_3 (l), then MeOH, ≈80%.

stereomers, proving that the homoallylic ether isomers **4b** differ in their configuration at C-4, ruling out (*RR*)-**4b**.

In another experiment, **4b** was treated with sodium in liquid ammonia to cleave the auxiliary moiety and to give homoallylic alcohols **7** (Scheme 4, b) which were found to be enantiomers. Thus, both initially formed homoallylic ether isomers have *anti* configuration, and the minor isomer has (*RS*)-configuration.

For the pentenylation, we performed the reaction with acetone and obtained an 84:16 mixture of diastereomers, which is almost identical to the 86:14 mixture obtained in the case of butanone. Since the acetone-derived products lack the stereogenic center in the 4-position, we conclude that the butanone-derived diastereomers differ in their configuration at C-3, which rules out (*RR*)-**4c** (the main isomer was assigned the (*RS*)-stereochemistry by X-ray analysis). In analogy to the crotylation, we therefore conclude that the minor isomer is the second *anti* isomer, namely (*SR*)-**4c**.

Thus, we found that the reaction is exclusively *anti*-selective in all cases, with a switch between main and minor isomer configuration when going from crotylation to pentenylation.

Conclusion

We have identified the TSs for the crotylation and pentenylation of butanone with the auxiliary (*S*,*S*)-**3**. The correct reproduction of the experimental behavior for three reactions implies that the correct TSs were found.

The relevant TSs for the three studied systems share the same conformations $\mathbf{A_3}$ and $\mathbf{B_3}$. The order of TSs is independent of the double bond geometry of the silane, but changes when crotyl silanes are substituted by pentenyl silanes. TS energies can be rationalized based on steric and electronic effects within the TS and on the different energies of solvation. The obtained reasoning can be extended to explain the selectivities obtained in hexenylations and heptenylations.

Experimental Section

Computational details: All calculations were performed with the Gaussian 03 program package.[11] TS geometries were initially identified by employing the semiempirical method AM1. Then, B3LYP/6-31+G(d)/PCM/UAKS[12,13] single-point energy calculations on the obtained geometries provided a list of TSs, of which only those with a relative energy of less than 15 kJ mol^{-1} were selected for further calculations. The relative energy is defined as the energy difference to the lowest-energy TS. In our previous study on the similar allylation reaction with the same oxocarbenium ion, we demonstrated that this approach does not neglect relevant TSs.[8] The TS geometries were reoptimized at the B3LYP/6-31+G(d)/PCM/UAKS level of theory with CH_2Cl_2 as solvent and setting the temperature to $T=195$ K, followed by a frequency calculation at the same level and for the same temperature. The nature of the TSs were validated by inspection of the eigenvalues of the Hessian matrices.

Employing transition state theory, we calculated the relative rate constants, k_{rel}, for every TS. Addition of the rate constants, k_{rel}, of all TSs leading to each of the four possible stereoisomers gave overall rate constants, the ratio of which corresponds to the predicted ratio of product isomers. In this respect, only TSs with a relative energy of less than 6 kJ mol^{-1} (termed "relevant TSs") may contribute more than 2% to the product formation in the limiting case of only one lower-energy TS. In all reported cases, there are more than one lower-energy TSs; consequently, higher-energy TSs can be neglected without any loss of accuracy.

For the calculation of activation energies, the TS energies were refined with single-point calculations by employing the larger basis set 6–311++G(2d,p). For selectivities, there was no significant change by using the larger basis set; all given relative TS energies G_{rel} were calculated with the 6-31+G(d) basis set.

Acknowledgements

This work has been supported by the Fonds der Chemischen Industrie. We thank the Gesellschaft für wissenschaftliche Datenverarbeitung Göttingen (GWDG) for providing access to their computing resources. T. K. acknowledges the Studienstiftung des deutschen Volkes for a PhD scholarship.

[1] a) S. E. Denmark, J. Fu, *Chem. Rev.* **2003**, *103*, 2763–2793; b) G. Majetich in *Organic Synthesis. Theory and Applications*, (Ed.: T. Hudlicky), JAI Press, Greenwich, CT, **1989**.

[2] a) M. Wadamoto, H. Yamamoto, *J. Am. Chem. Soc.* **2005**, *127*, 14556–14557; b) R. Wada, K. Oisaki, M. Kanai, M. Shibasaki, *J. Am. Chem. Soc.* **2004**, *126*, 8910–8911; c) J. R. Huckins, S. D. Rychnovsky, *J. Org. Chem.* **2003**, *68*, 10135–10145; d) K. M. Waltz, J. Gavenonis, P. J. Walsh, *Angew. Chem.* **2002**, *114*, 3849–3852; *Angew. Chem. Int. Ed.* **2002**, *41*, 3697–3699; e) M. Nakamura, A. Hirai, M. Sogi, E. Nakamura, *J. Am. Chem. Soc.* **1998**, *120*, 5846–5847; f) D. Sames, Y. Liu, L. DeYoung, R. Polt, *J. Org. Chem.* **1995**, *60*, 2153–2159; g) A. Mekhalfia, I. E. Markó, *Tetrahedron Lett.* **1991**, *32*, 4779–4782; h) K. Soai, M. Ishizaki, *J. Org. Chem.* **1986**, *51*, 3290–3295; i) H. Roder, G. Helmchen, E. Peters, K. Peters, H. von Schnering, *Angew. Chem.* **1984**, *96*, 895–896; *Angew. Chem. Int. Ed. Engl.* **1984**, *23*, 898–899.

[3] a) L. F. Tietze, *Chem. Rev.* **1996**, *96*, 115–136; b) L. F. Tietze, G. Brasche, K. Gericke, *Domino Reactions in Organic Synthesis*; 1st ed.; Wiley VCH: Weinheim **2006**.

[4] a) L. F. Tietze, K. Schiemann, C. Wegner, *J. Am. Chem. Soc.* **1995**, *117*, 5851–5852; b) L. F. Tietze, B. Weigand, L. Völkel, C. Wulff, C. Bittner, *Chem. Eur. J.* **2001**, *7*, 161–168; c) L. F. Tietze, K. Schiemann, C. Wegner, C. Wulff, *Chem. Eur. J.* **1998**, *4*, 1862–1869; d) L. F. Tietze, S. Hölsken, J. Adrio, T. Kinzel, C. Wegner, *Synthesis* **2004**, *13*, 2236–2239; e) L. F. Tietze, C. C. Brazel, S. Hölsken, J. Magull, A. Ringe, *Angew. Chem.* **2008**, *120*, 5324–5327; *Angew. Chem. Int. Ed.* **2008**, *47*, 5246–5249.

[5] a) A. J. Birch, *J. Chem. Soc.* **1944**, 430–436; b) P. W. Rabideau, Z. Marcinow, *Org. React.* **1992**, *42*, 1–334.

[6] L. F. Tietze, L. Völkel, C. Wulff, B. Weigand, C. Bittner, P. McGrath, K. Johnson, M. Schäfer, *Chem. Eur. J.* **2001**, *7*, 1304–1308.

[7] L. F. Tietze, T. Kinzel, S. Schmatz, *J. Am. Chem. Soc.* **2006**, *128*, 11483–11495.

[8] L. F. Tietze, T. Kinzel, S. Schmatz, *J. Am. Chem. Soc.* **2008**, *130*, 4386–4395.

[9] a) K. Manju, S. Trehan, *Chem. Commun.* **1999**, 1929–1930; b) M. Paddon-Row, N. G. Rondan, K. N. Houk, *J. Am. Chem. Soc.* **1982**, *104*, 7162–7166; c) J. L. Broeker, R. W. Hoffmann, K. N. Houk, *J. Am. Chem. Soc.* **1991**, *113*, 5006–5017; d) S. E. Denmark, E. J. Weber, *J. Am. Chem. Soc.* **1984**, *106*, 7970–7971; e) S. E. Denmark, T. M. Willson, *J. Am. Chem. Soc.* **1989**, *111*, 3475–3476; f) S. E. Denmark, N. G. Almstead, *J. Org. Chem.* **1994**, *59*, 5130–5132; g) S. E. Denmark, H. Hosoi, *J. Org. Chem.* **1994**, *59*, 5133–5135;

h) A. Bottoni, A. L. Costa, D. Di Tommaso, I. Rossi, E. Tagliavini, *J. Am. Chem. Soc.* **1997**, *119*, 12131–12135.

[10] For the employed elimination using 2-nitrophenyl selenocyanate, see P. A. Grieco, S. Gilman, M. Nishizawa, *J. Org. Chem.* **1976**. *41*, 1485–1486.

[11] Gaussian 03, Revision B.04, M. J. Frisch, G. W. Trucks, H. B. Schlegel, G. E. Scuseria, M. A. Robb, J. R. Cheeseman, J. A. Montgomery, Jr., T. Vreven, K. N. Kudin, J. C. Burant, J. M. Millam, S. S. Iyengar, J. Tomasi, V. Barone, B. Mennucci, M. Cossi, G. Scalmani, N. Rega, G. A. Petersson, H. Nakatsuji, M. Hada, M. Ehara, K. Toyota, R. Fukuda, J. Hasegawa, M. Ishida, T. Nakajima, Y. Honda, O. Kitao, H. Nakai, M. Klene, X. Li, J. E. Knox, H. P. Hratchian, J. B. Cross, C. Adamo, J. Jaramillo, R. Gomperts, R. E. Stratmann, O. Yazyev, A. J. Austin, R. Cammi, C. Pomelli, J. W. Ochterski, P. Y. Ayala, K. Morokuma, G. A. Voth, P. Salvador, J. J. Dannenberg, V. G. Zakrzewski, S. Dapprich, A. D. Daniels, M. C. Strain, O. Farkas, D. K. Malick, A. D. Rabuck, K. Raghavachari, J. B. Foresman, J. V. Ortiz, Q. Cui, A. G. Baboul, S. Clifford, J. Cioslowski, B. B. Stefanov, G. Liu, A. Liashenko, P. Piskorz, I. Komaromi, R. L. Martin, D. J. Fox, T. Keith, M. A. Al-Laham, C. Y. Peng, A. Nanayakkara, M. Challacombe, P. M. W. Gill, B. Johnson, W. Chen, M. W. Wong, C. Gonzalez, and J. A. Pople, Gaussian, Inc., Pittsburgh PA, **2003**.

[12] a) A. D. Becke, *Phys. Rev. A* **1988**, *38*, 3098–3100; b) C. Lee, W. Yang, R. G. Parr, *Phys. Rev. B* **1988**, *37*, 785–789; c) A. D. Becke, *J. Chem. Phys.* **1993**, *98*, 5648–5652.

[13] a) B. Mennuci, R. Cammi, J. Tomasi, *J. Chem. Phys.* **1999**, *110*, 6858–6870; b) M. Cossi, G. Scalmani, N. Rega, V. Barone, *J. Chem. Phys.* **2002**, *117*, 43–54.,

Received: September 14, 2008
Published online: January 2, 2009

